ELSEVIER

Contents lists available at ScienceDirect

## Current Research in Biotechnology

journal homepage: www.elsevier.com/locate/crbiot





# Anti-Melanoma efficacy of traditional multi-herbal extracts from mongolian ethnomedicine on B16F10 murine cells

Yerkegul Dauletkhan <sup>a,b</sup>, Tae Young Han <sup>c</sup>, Janbolat Ashim <sup>d</sup>, Shukherdorj Baasanmunkh <sup>e</sup>, Altantsetseg Khajidsuren <sup>a</sup>, Wookyung Yu <sup>d</sup>, Purevjargal Naidansuren <sup>f</sup>, Uteubayeva Gulzada <sup>b</sup>, Kang Duk Choi <sup>c</sup>, Baatartsogt Oyungerel <sup>a,\*</sup>

- <sup>a</sup> School of Animal Science and Biotechnology, Mongolian University of Life Sciences, Ulaanbaatar, 17024, Mongolia
- <sup>b</sup> Department of Immunology, Astana Medical University, Nur-Sultan, 010000, Republic of Kazakhstan
- <sup>c</sup> Genomic Informatics Center, Hankyong National University, Anseong, 456-749, Republic of Korea
- <sup>d</sup> Department of Brain Sciences, DGIST, Daegu, 42988, Republic of Korea
- <sup>e</sup> Department of Biology & Chemistry, Changwon National University, Changwon 51140, Republic of Korea
- f Mon-CL Fertility Center, Ulaanbaatar, 17011, Mongolia

#### ARTICLE INFO

#### Keywords: Ethnopharmacology Melanoma G4 extract Apoptosis Xenograft models

#### ABSTRACT

Multi-herbal formulation is an attractive approach to developing novel therapeutic strategies to manage advanced forms of melanoma. This research aims to evaluate the anti-melanoma potential of Traditional Multi-Herbal (G4) Extracts sourced from Mongolian Ethnomedicine utilizing both cellular and xenograft models. In vitro and ex vivo experiments employing B16F10 melanoma cells were conducted to evaluate the anti-cancer effect of the G4 extract. Furthermore, in vivo experiments utilizing BALB/C nu/nu mice xenograft models were carried out to gauge the extract's effectiveness. A comprehensive analysis encompassing various assays, such as cell viability, migration and invasion assays, cellular phase analysis, and key indicators of apoptosis, was performed. These indicators included activation of the caspase-3 cascade, genomic DNA fragmentation, nuclear staining alterations, and levels of cell cycle and apoptotic regulatory markers analysis. Our Results showed that the G4 extract exhibited potent anti-cancer effects on B16F10 melanoma cells, notably inhibiting cell migration and vascular sprouting in a concentration-dependent manner, suggesting its potential to impede melanoma metastasis. This investigation underscores the promising anti-cancer potential of the G4 extract against melanoma cells through the modulation of apoptotic pathways and suppression of tumor xenograft growth. Ultimately, our findings suggest that the G4 extract holds promise as a candidate for the development of future melanoma chemotherapeutics.

#### 1. Introduction

Melanoma, a metastatic and highly aggressive type of skin cancer, poses a significant global health burden (Gray-Schopfer et al., 2007; Erdei and Torres, 2010). The incidence of melanoma has consistently risen globally over the past few decades (Antohe et al., 2019; Arnold et al., 2022). Each year, approximately 232,100 cases of newly diagnosed primary malignant cancers (excluding non-melanoma skin cancer) are attributed to cutaneous melanoma, resulting in roughly 55,500 cancer-related deaths (Dirk Schadendorf et al., 2018). The capacity of melanoma to metastasize to vital organs, such as the lungs, liver, brain, and lymph nodes, significantly contributes to its high mortality and

morbidity rates (Antohe et al., 2019). Addressing these challenges necessitates the discovery of more effective strategies to enhance the survival rates of melanoma patients. In this regard, traditional medicinal plants have garnered interest as potential alternatives for tackling aggressive cancer forms (Cragg and Newman, 2005; Halder et al., 2015; Wang et al., 2015; Kim et al., 2016). Recently, researchers have pinpointed numerous plants that manifest anti-cancer properties, emphasizing those employed in herbal medicine in developing nations (Wang et al., 2015; Bao et al., 2016; Purushotham et al., 2016; Qamar et al., 2022). Multiple studies have explored the effects of herbal products against cancer cells, revealing a variety of mechanisms of action. For example, natural products derived from *Forsythiae Fructus* curtail

E-mail address: baatartsogt@muls.edu.mn (B. Oyungerel).

<sup>\*</sup> Corresponding author.

cellular proliferation via the MAPKs/HO-1 signaling pathway (Wang et al., 2015; Bao et al., 2016). In contrast, the methanolic extract from *Ganoderma lucidum* showcases antioxidant and anti-inflammatory activities that induce caspase-dependent apoptosis, upregulate p53-mediated cell death, and suppress Bcl-2 expression (Harhaji Trajkovic et al. (2009); Barbieri et al., 2017). Extracts from *Taohong siwu* demonstrate anti-angiogenic characteristics by downregulating VEGF expression, while *Spatholobus suberectus* extracts impede cancer cell adhesion, invasion, migration, and metastasis (Tang et al., 2021; Kiddane et al., 2022).

Traditional Japanese (Kampo) and Chinese traditional medicine (TCM) have been employed for thousands of years in disease management, health maintenance, and prolonging life expectancy in Asian countries such as China, Mongolia, and Korea (Iwase et al., 2012; Šmejkal et al., 2016; Soares et al., 2019; Wurchaih and Menggenqiqig (2019)). Chinese herbal medicine (CHM), a fundamental component of TCM, utilizes combinations of up to 20 herbs in intricate formulations (Zhou et al., 2016). Additionally, the 15th-century book "Shipagerlik Bayan" authored by Kazakh medical doctor Oteyboydak Tleukabyl, offers an in-depth exploration of ethnomedicinal plants, formulations, and dietary practices within Traditional Kazakh Medicine (TKM) (Dzhumagaliyeva et al., 2020; Nurlybekova et al., 2022). In this study, we selected four traditional medicinal plants, namely, Artemisia glabella Kar. & Kir. (synonym of Artemisia obtusiloba var. glabra Lebeb) (Asteraceae), Dasiphora fruticosa (L.) Rydb. (Rosaceae), Paeonia anomala L. (Paeoniaceae), and Zygophyllum potaninii Maxim. (Zygophyllaceae), to prepare a multi-herbal formulation. The selection of these plants is grounded in their traditional medicinal applications in Mongolian folk medicine (MFM) and traditional Kazakh medicine (TKM) (Tsevegsuren et al., 2007; Šmejkal et al., 2016; Soares et al., 2019; Wurchaih and Menggenqiqig (2019)). Ethnomedicinal formulas as G4 inherits the essence of treating diseases and saving lives from generation to generation. Previous research studies have explored individual plants within G4, employing modern research methodologies such as molecular biology and phytochemistry, albeit with a limited number of studies available. For instance, extracts of Artemisia glabella have been utilized for gastrointestinal tract and liver diseases, cancer, antidotes, and various skin and mucous membrane diseases (Feng et al., 2020). Different extracts from the aerial or underground parts of Dasiphora fruticosa have been traditionally used to address inflammation, wounds, and certain forms of cancer (Tomczyk and Latté (2019); Kumari et al., 2021). Moreover, Paeonia anomala and Zygophyllum potaninii are recognized ethnomedicinal plants in MFM, employed to treat various conditions including inflammation and abdominal pain (Bayarmaa et al., 2018; Yang et al., 2020; Gendaram, 2017). Also, recently phytochemical constituents and pancreatic lipase inhibitory activities from aerial part of Paeonia anomala were reported (Purevdorj E, 2018). The four herbal extracts, termed G4, were formulated drawing on the ethnobotanical knowledge associated with the selected herbs. Consequently, the limited characterizations of the G4 formulation under modern research approaches enable us to investigate its anticancer effects from a molecular biological perspective. The primary objective of this study is to assess the anticancer potential of the G4 formula on the murine B16F10 melanoma cell line and xenograft model using a variety of independent assays. These assays encompass cell viability, wound healing, aortic ring assay, cellular migration and invasion assays, cellular phase evaluations, nuclear staining, DNA fragmentation assay, and western blotting. Through comprehensive examination of the effects of the G4 formula, we aim to offer insights into its potential as a therapeutic intervention for melanoma.

## 2. Materials and methods

## 2.1. Plant material and extract preparation

In this study, we selected four medicinal plants: Artemisia glabella

Kar. & Kir. (synonymous with Artemisia obtusiloba var. glabra Lebeb), Dasiphora fruticosa (L.) Rydb., Paeonia anomala L., and Zygophyllum potaninii Maxim from Mongolia. The author and species names of these chosen plants are consistent with the latest checklist of Mongolian flora (Baasanmunkh et al., 2022). These selected species are generally found in the forest-steppe and steppe regions of Mongolia (Baasanmunkh et al., 2022), except Z. potaninii. Notably, Z. potaninii grows in the desert and desert steppe regions in the southern part of the country (Baasanmunkh et al., 2022). The herbal materials for each species used in this study were sourced from the plant collection at the School of Animal Science and Biotechnology, Mongolian University of Life Sciences. The original herbarium materials for each species were deposited in the herbarium of the National University of Mongolia. The voucher information for all species is as follows: Artemisia glabella (UBU34072), Dasiphora fruticosa (UBU34073), Paeonia anomala (UBU34074), and Zygophyllum potaninii (UBU34075). The multi-herbal extract (G4) was prepared from the four aforementioned medicinal plants, based on their ethnomedicinal significance. For the extraction process, we opted for 40 % ethanol due to its general recognition as safe for consumption and usage in ethnomedicine. To prepare the extract, the entire parts of the medicinal herbs were dried and subsequently ground into a powder (Labconco, USA). The powdered herbs were combined in equal amounts (0.5 kg) by dry weight and immersed in 40 % ethanol, totalling 2L in volume. This mixture was soaked for 24 h. Post-soaking, the residual portion was separated by centrifugation at 5,000 rpm for 15 min, and the resultant solution was then filtered using Whatman no. 1 filter paper. The acquired ethanol extract was concentrated with a rotary evaporator (Büchi, Switzerland) set at 50 °C and 60 rpm (Bak et al., 2006). Following this, the concentrated extract underwent freeze-drying to achieve a powdered state. The freeze-dried extract was reconstituted in dimethyl sulfoxide (DMSO) at a stock concentration of 100 mg/mL, then kept at 4 °C until to produce an appropriate solution for cell culture and subsequent experiments.

#### 2.2. Cell line and culture

B16F10 and HaCaT cells were cultured in Dulbecco's Modified Eagle's Medium (DMEM) supplemented with 10 % fetal bovine serum (FBS) and penicillin/streptomycin (100 U/ml). The cell cultures were maintained at 37  $^{\circ}\text{C}$  in a humidified atmosphere with 5 % CO<sub>2</sub>.

#### 2.3. Cell viability assay

The cytotoxicity of the G4 extract was assessed using the Cell Counting Kit-8 assay (Dojindo Laboratories, Tokyo, Japan). B16F10 and HaCaT cells were seeded in 96-well plates at a density of  $1\times10^4$  cells per well. After 12 h of incubation at 37  $^{\circ}\text{C}$ , the cells were treated with varying concentrations (0.031, 0.062, 0.125, 0.25, 0.5, 1, and 2 mg/ml) of the G4 extract and then incubated for an additional 24 and 48 h at 37  $^{\circ}\text{C}$ . Post-incubation, 10  $\mu\text{L}$  of CCK-8 solution was added to each well and the plates were incubated for another four h at 37  $^{\circ}\text{C}$ , following the protocol described by Kim et al. (2022). The absorbance was measured at 450 nm using a microplate reader (SpectraMax iD3, Molecular Devices, CA, USA).

## 2.4. In-vitro wound healing assay

B16F10 cells were seeded in six-well plates at a density of  $5\times 10^5$  cells/ml and cultured overnight at 37 °C to ensure attachment and growth. An in-vitro wound was then created in the cultured monolayer using a 10  $\mu L$  micropipette tip, following treatment of the cells with various concentrations of the G4 extract (Kim et al., 2023). Cell migration was monitored over a 24-hour period using time-lapse imaging with an optical microscope (Olympus, CK40-32PH, Tokyo, Japan) in the presence of serum-containing medium, maintained at 37 °C. Images were taken at six-hour intervals, and the average number of migrated

cells was tallied. Graphs representing the migration data were constructed using Prism5 software.

#### 2.5. Trans-well invasion assay

Cell invasion assays were conducted using trans-well plates equipped with an 8 µm pore size and a polyethylene terephthalate (PET) membrane. Each trans-well insert was loaded with 100 ul of Matrigel (BD Biosciences, Bedford, MA, USA) and permitted to solidify in a 5 % CO2 incubator at 37 °C for two h. In the lower compartment of the *trans*-well plate, 0.6 ml of DMEM supplemented with 10 % fetal bovine serum (FBS) was added. B16F10 cells were seeded at a density of 1x10<sup>5</sup> cells/ well in serum-free DMEM and introduced into the upper compartment of the trans-well plate. These cells were treated with varying concentrations of G4 extract and incubated in a 5 % CO2 incubator at 37 °C for 16 h. Non-invading cells on the upper surface of the trans-well membrane were removed by gentle swabbing with cotton. Cells that penetrated to the lower surface of the membrane were fixed using methanol and stained with Gemsia (Pijuan et al., 2019). Subsequently, they were visualized and captured using an inverted optical microscope (Nikon, Japan). The extent of invasion was evaluated by tallying the stained cells across three randomly chosen high-power (100x) fields.

#### 2.6. Rat aortic rings assay

Eight-well tissue culture plates were coated with 100  $\mu$ L of Matrigel (BD Biosciences, MA, USA) and allowed to solidify for two h at 37 °C in a 5 % CO<sub>2</sub> incubator. Thoracic aortas were sourced from 10-week-old male Sprague Dawley rats. After the removal of fibro-adipose tissues, the aortas were segmented into 1-mm long cross-sections using a surgical blade. Each aortic cross-section was placed onto the Matrigel-coated wells, covered with an additional 100  $\mu$ L of Matrigel and incubated for 30 min at 37 °C in a 5 % CO<sub>2</sub> incubator (Bellacen and Lewis, 2009). VEGF (20 ng/mL), along with various concentrations of G4 (0.125, 0.25, 0.5 mg/mL), was added to the wells. On the 9th day, images of the rings were captured at 200x magnification. The degree of angiogenic sprouting, micro-vessel outgrowth from rings was quantified using the ImageJ software (Schneider et al., 2012). The experiments were conducted in triplicate to ensure the consistency and reproducibility of the results.

## 2.7. Measurement of apoptosis

Cells were cultured in 6-well plates at a seeding density of  $5\times10^5$  cells/well and were treated with various concentrations of G4 extract (0.125, 0.25, and 0.5 mg/ml). After a 24-hour treatment period, the cells

were harvested and washed twice with PBS. The collected cells were then stained using the Annexin V-FITC apoptosis kit (BD Biosciences) in accordance with the manufacturer's instructions. Flow cytometry analysis was conducted using the CellQuest software, with the Annexin V-FITC fluorescence emission being measured to assess apoptosis.

#### 2.8. Nuclear staining

Apoptosis induced in G4-treated cells was fixed with 4 % paraformaldehyde in 1x PBS. After washing with 1x PBS, the cells were stained using ProLong Gold Antifade reagent containing 4′,6-diamidino2-phenylindole (DAPI; Invitrogen, CA, USA). Nuclear condensation and fragmentation were subsequently visualized with a fluorescence microscope.

#### 2.9. Genomic DNA fragmentation analysis

B16F10 melanoma cells were cultured and treated with G4 extract, as described in the previous section. After treatment, cells were incubated for 24 h at 37 °C, harvested, and rinsed with PBS. The resulting cell pellets were lysed using a solution containing 10 mM Tris HCl (pH 8.0), 10 mM EDTA, and 0.5 % Triton X-100. These lysates underwent digestion with 0.1 mg/mL RNase A at 37 °C for 1 h. Following this, the samples were centrifuged at 12,000 rpm for 25 min to pellet chromosomal DNA (Majtnerová and Roušar, 2018). The supernatant, which contains digested cellular proteins, was treated with 1 mg/mL proteinase K at 50 °C for 2 h in the presence of 1 % sodium dodecyl sulfate. DNA was then extracted using a phenol–chloroform mixture and precipitated with cold ethanol. The isolated DNA fragments were electrophoretically separated on 1.5 % agarose gels infused with ethidium bromide. Gels were visualized under UV light transillumination, and images were acquired using a computer-assisted image processor.

## 2.10. Western blotting

For immunoblotting, proteins from 12 % SDS gels were transferred to nitrocellulose transfer membranes and blocked with 5 % skim milk in 1x TBST blocking solution. Primary antibodies against PARP, p-p53, caspase 3, cyclin B1, cyclin D1, cyclin D3, CDK2, p-Erk1/2, p-MEK (Cell Signaling Technology, Inc. USA), and GAPDH (Santa Cruz Biotechnology, Inc., Santa Cruz, CA) were used. Horseradish peroxidase-conjugated mouse or rabbit IgG antibodies served as secondary antibodies. Protein detection was carried out using the Amersham  $^{\rm TM}$  ECL  $^{\rm TM}$  Prime Western Blotting Reagent Kit (GE Healthcare, Italy) for enhanced chemiluminescence (ECL) detection.

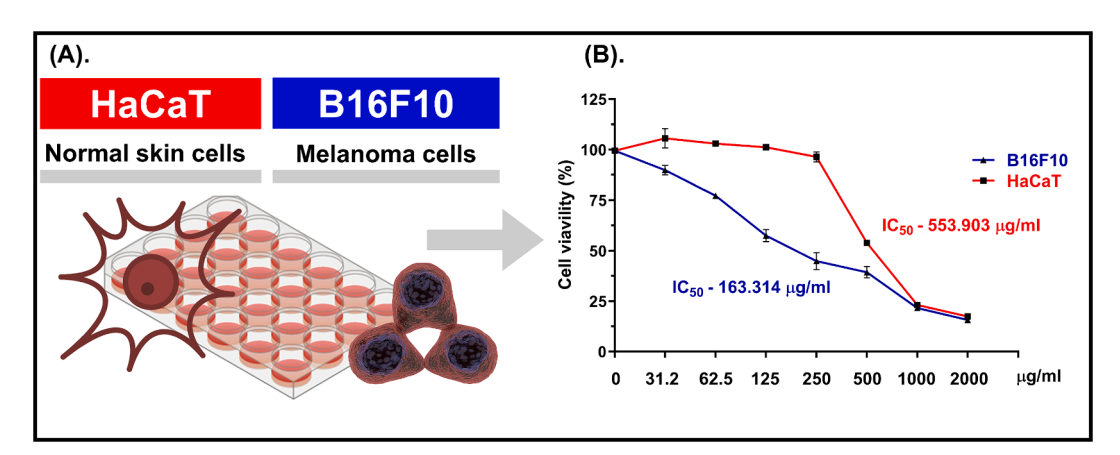


Fig. 1. Cell viability comparisons. (A) Schematic representations of cell viability test. (B) Cell viability comparison between of B16F10 and HaCaT cells. Data are represented as mean  $\pm$  SD values from three independent replicates, each performed in triplicate. \*, P < 0.05; \*\*, P < 0.01; \*\*\*, P < 0.001; \*\*\*\*, P < 0.0001; ns, non-significantly different compared to untreated controls.

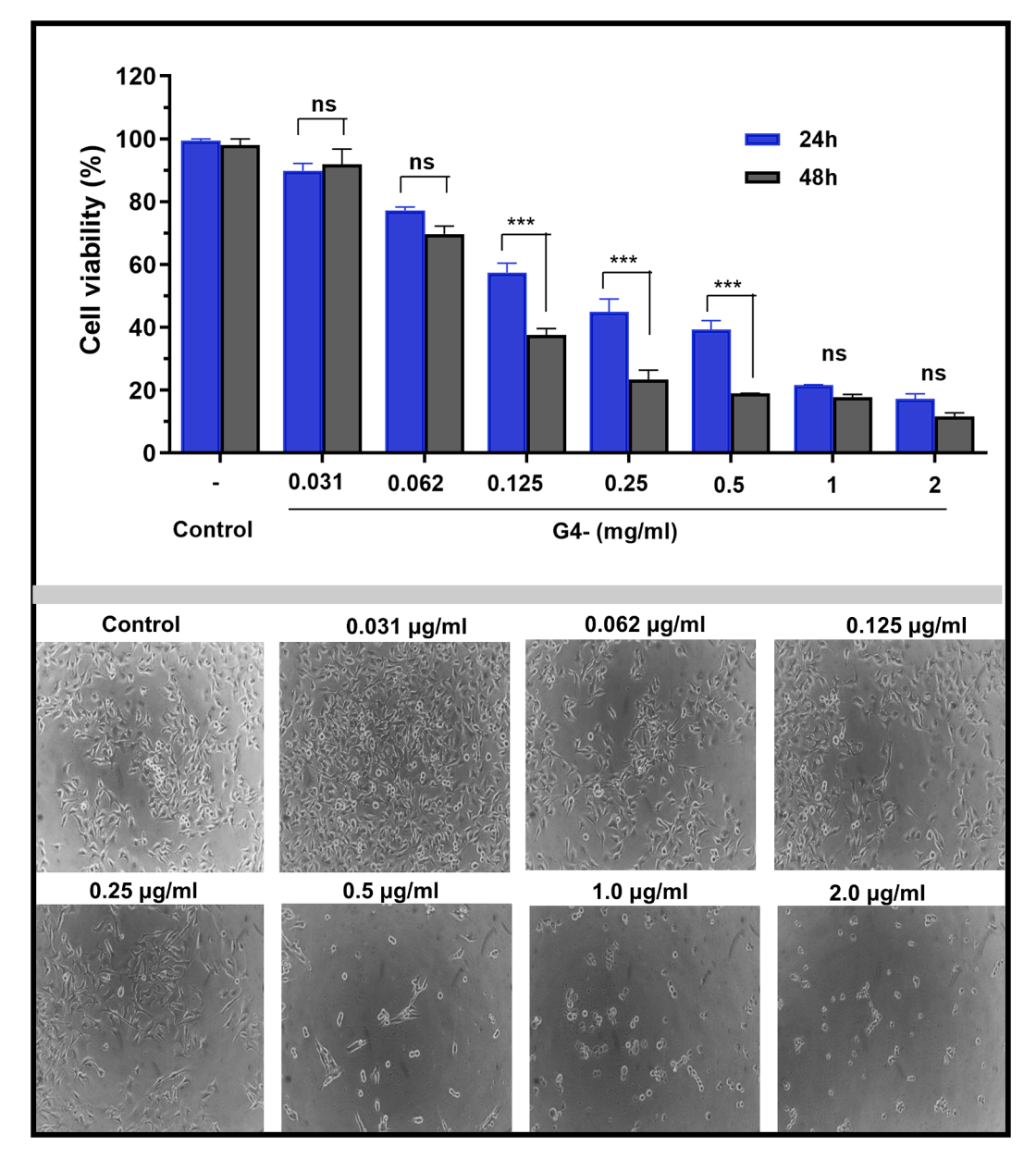


Fig. 2. Dose and time-dependent analysis of cell viability in B16F10 cells. (A) G4 inhibited the cell viability of B16F10 cells in a dose and time-dependent manner. Data are represented as mean  $\pm$  SD values from three independent replicates, each performed in triplicate. \*, P < 0.05; \*\*, P < 0.01; \*\*\*\*, P < 0.001; \*\*\*\*, P < 0.0001; ns, non-significantly different compared to untreated controls.

## 2.11. Animals and xenograft analysis

Six weeks old male BALB/C nu/nu mice (n = 16) were procured from Nara BioTech Co., LTD. (Korea). Throughout the experiment, the mice were housed in plastic cages at a controlled temperature of  $22\pm2\,^{\circ}\text{C}$ , under a 12-hour light/dark cycle, and were given ad libitum access to both food and water. All measures were taken to minimize the discomfort experienced by the animals and to reduce the total number of animals utilized. For the xenograft analysis, male BALB/C nu/nu mice, aged 6–8 weeks, were inoculated with B16F10 cells. Specifically,  $1\times10^6$  cells in 0.5 mL of serum-free DMEM were subcutaneously injected into the flanks of each mouse. The development of tumors was monitored, and mice were euthanized at pre-established intervals. Tumor volume was determined using an external calliper and calculating the volume using the equation,  $V=0.5233\times10^{12}$  length x width2. The volumes were plotted, and statistical analysis was performed. All animal care and experimental procedures strictly adhered to the guidelines for the care

and use of laboratory animals, in accordance with the ethical standards set by Hankyong National University.

## 2.12. Statistical analysis

Statistical significance for all experiments was assessed using a one-way analysis of variance (ANOVA), followed by Tukey's multiple comparison test. Results were deemed statistically significant when the significance level was  $p<0.05. \label{eq:policy}$ 

## 3. Results

## 3.1. G4 treatment inhibited cell viability in B16F10 melanoma cells

The effect of G4 on the B16F10 melanoma and HaCaT cell line was first evaluated using a Cell Counting Kit-8 (CCK-8) assay. Cells were treated with various G4 concentrations (0.031, 0.062, 0.125, 0.25, 0.5,

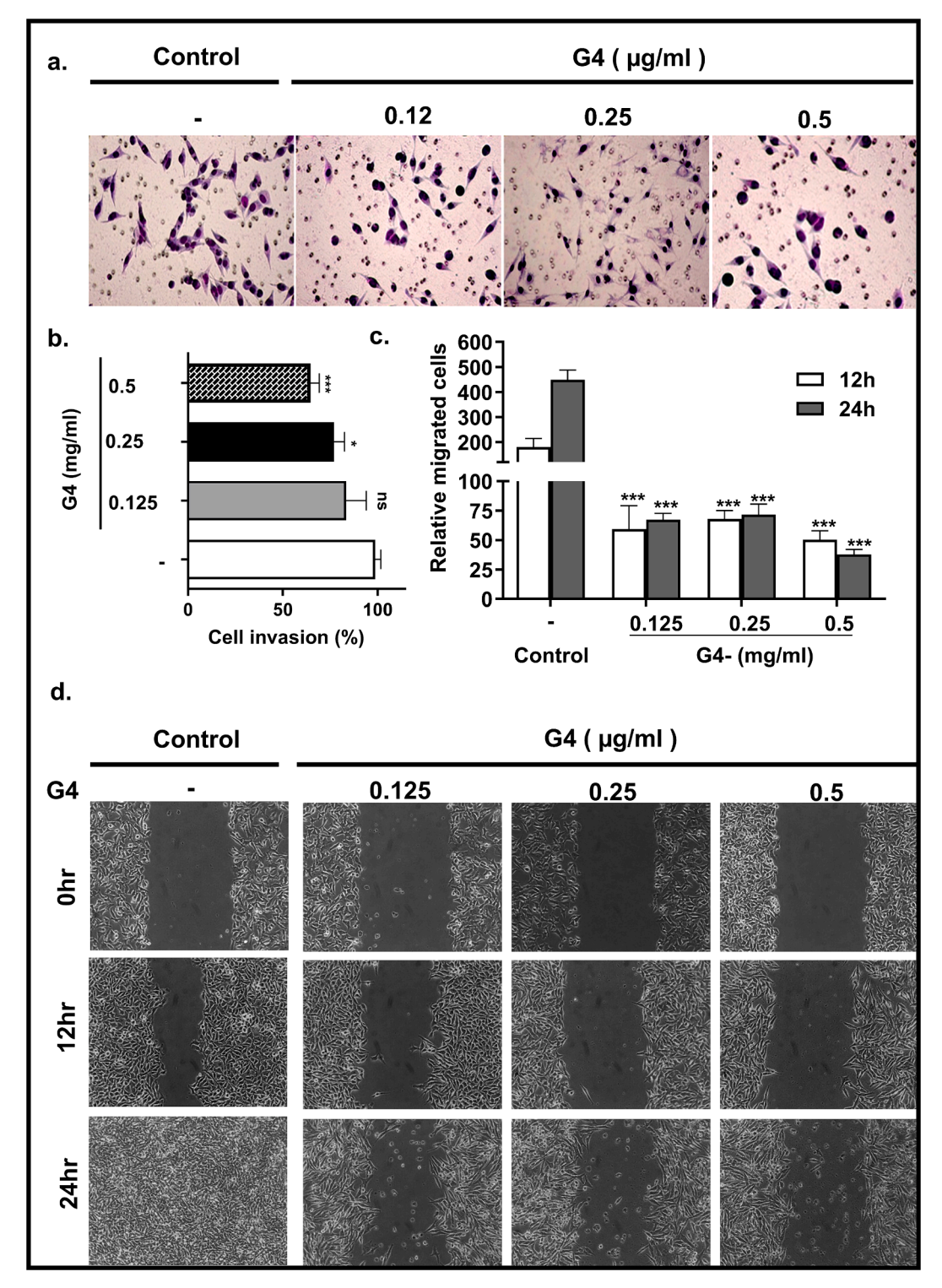
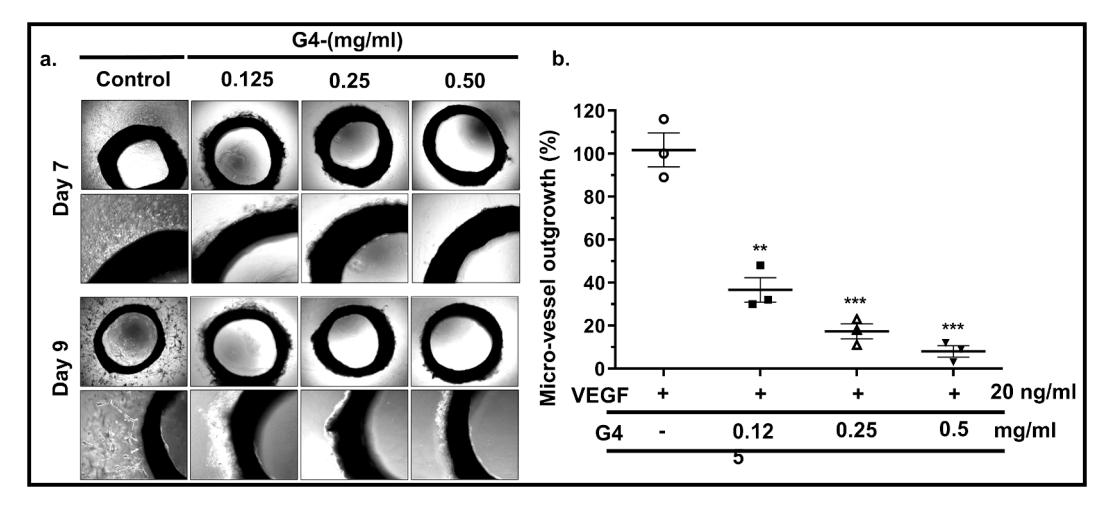


Fig. 3. Cells migration and Invasion analysis. Representative images of *trans*-well assays and average numbers of cells (A and B) Representative images of scratch assay and quantitative analysis (C and D). Data are represented as mean  $\pm$  SD values from three independent replicates, each performed in triplicate. \*, P < 0.05; \*\*, P < 0.01; \*\*\*, P < 0.001; \*\*\*\*, P < 0.001; \*\*\*\*, P < 0.0001; ns, non-significantly different compared to untreated controls.

1, and 2 mg/mL) and incubated for 24 at 37 °C. The results exhibited a significant (\*p < 0.0001; Fig. 1 A) dose-dependent inhibition of B16F10 melanoma cell compared to normal skin keratinocyte cells The half-maximum inhibitory concentration (IC50) was determined to be 163.31  $\mu g/mL$  in B16F10 melanoma cells and 553.9  $\mu g/mL$  in normal skin keratinocyte cells (Fig. 1), suggesting a potential selective inhibition of melanoma cells by G4 treatment. Next, we examined the dose

dependency response using B16F10 melanoma cells with extended time points for 48 h. In this experiment, G4 treatment dose dependently inhibited the growth of B16F10 melanoma cells. In particular, concentrations of G4 at 0.125, 0.25, and 0.5 mg/mL demonstrated marked significant effect in B16F10 melanoma cells (Fig. 2 A). Consequently, we opted to utilize these concentrations (0.125, 0.25, and 0.5 mg/mL) for subsequent investigations.



**Fig. 4.** Inhibition of in vitro angiogenesis by G4, evaluated using the rat aortic ring assay. (A) Representative images depicting micro-vessel outgrowths captured by phase-contrast microscopy after 7 and 9 days of incubation. (B) Quantification of micro-vessel outgrowths. Values are represented as mean  $\pm$  3 SD (from triplicate measurements). \*, P < 0.05; \*\*\*, P < 0.01; \*\*\*\*, P < 0.001; \*\*\*\*, P < 0.0001; ns, non-significantly different compared to untreated controls.

#### 3.2. Inhibition effects of G4 on B16F10 melanoma cell migration

Invasion and cell migration refer to the movement of cells from one location to another. In cancer, this process is crucial for the spread of cancer cells from the primary tumor to surrounding tissues and distant organs, leading to metastasis (Chambers et al., 2002). We investigated the impact of G4 on the migratory and invasive capacities of B16F10 melanoma cells. B16F10 melanoma cells were exposed to varying concentrations of G4 (0.125, 0.25, and 0.5 mg/mL), after which the effects on invasion and migration were evaluated. Our results demonstrated a significant (\*p < 0.05) reduction in invasion by the B16F10 melanoma cells at a G4 concentration of 0.25 mg/mL (Fig. 3 A and B) in 24 h treatment compared to control group.

Additionally, G4 demonstrated notable inhibition of B16F10 melanoma cell migration at concentrations of 0.125, 0.25, and 0.5 mg/mL (Fig. 3 C and D). Crucially, these inhibitory effects were observed to escalate in a dose-dependent and time-dependent fashion, suggesting that increased G4 concentrations have a more profound suppressive effect on the invasion and migration potential of B16F10 melanoma cells. These findings suggest that G4 may possess anti-metastatic properties, potentially limiting the spread of B16F10 melanoma. Building upon this observation, we proceeded to confirm the anti-metastatic potential of the G4 extract through experiments conducted under the *ex-vivo* conditions using the aortic rings assay.

## 3.3. Effect of G4 on ex-vivo angiogenesis

To assess the influence of G4 on micro-vessel outgrowth, we carried out an *ex-vivo* aortic rings assay. As expected, the introduction of VEGF (20 ng/mL) prominently promoted micro-vessel sprouting around the aortic rings, as shown in Fig. 4 A. Intriguingly, aortic rings treated with G4 displayed a marked reduction in micro-vessel outgrowths compared to the control rings (\*p < 0.05). The administration of G4 led to significant suppression of micro-vessel formation, as illustrated in Fig. 4 A. In particular, the G4 extract, at a concentration of 0.5 mg/mL, entirely halted the VEGF-induced micro-vessel sprouting in rat aortic rings. These results suggest that G4 has a suppressive effect on capillary sprouting from the rat aortic rings, underscoring its potential antiangiogenic properties.

## 3.4. Descriptions of apoptotic features

Based on the results described above, we next examined the various established independent indicators of apoptosis, specifically the

translocation of phosphatidylserine from the inner to the outer leaflet of the plasma membrane (Galluzzi et al., 2018), utilizing Annexin-V staining and induction of cell membrane permeabilization using propidium iodide (PI), cellular morphogen, nuclear condensation, genomic DNA fragmentations in the B16F10 cells. Subsequent flow cytometric analysis was employed to assess apoptosis in both G4-treated and untreated B16F10 melanoma cells. The outcomes revealed pronounced alterations in cell morphology and fluorescent DNA labeling in G4-treated B16F10 melanoma cells, pointing to evident DNA fragmentation (Fig. 5 A and D). Notably, marked morphological differences were observed in B16F10 cells post-G4 treatment relative to the control group. Post-exposure to varied G4 concentrations, the cells displayed a contracted appearance and evident chromatin condensation (Fig. 5 A).

These observations indicate that G4 treatment prompts considerable changes in cell morphology nuclear condensation, and genomic DNA fragmentation, hallmarks of apoptotic processes in B16F10 melanoma cells. This suggest that G4 treatment initiates apoptosis. For that reason, to measure the number of Annexin-V positive, PI positive cells by flow cytometry. (Fig. 5 B and C). Together, these analyses consistently demonstrate the induction of apoptosis in melanoma cells by G4.

## 3.5. G4 modulates apoptotic protein expression in a dose- and Time-Dependent manner

To elucidate the mechanism behind G4-induced apoptosis and its influence on cell cycle regulatory proteins, we conducted a western blot analysis. This was to observe changes in protein expression in B16F10 melanoma cells after treatments that varied in dose and duration. We inspected the expression levels of pro-apoptosis regulatory proteins, notably cleaved-PARP, p-p53, and cleaved-caspase-3. The western blot analysis of lysates from B16F10 cells (Fig. 6 A) highlighted an augmented expression of cleaved-PARP, p-p53, and activated caspase-3 in a manner that was both dose and time-dependent post-G4 treatment, three markers of apoptosis (Fig. 6 A). This data suggests that G4 treatment amplifies the expression of pro-apoptosis proteins, implying its role in advancing apoptosis in B16F10 melanoma cells.

Additionally, we assessed the protein levels of several cell cycle regulatory proteins, such as cyclin B1, cyclin D1, cyclin D3, cyclin E, and CDK-2, in B16F10 melanoma cells post-treatments that varied based on time and dosage. Our observations (Fig. 6 B) indicated that the G4 treatment diminished the expression of cyclin B1, cyclin D1, cyclin D3, cyclin E, and CDK-2 relative to the control group. This data implies that the G4 extract modulates the expression levels of cell cycle regulatory proteins in B16F10 melanoma cells. In summation, our results indicate

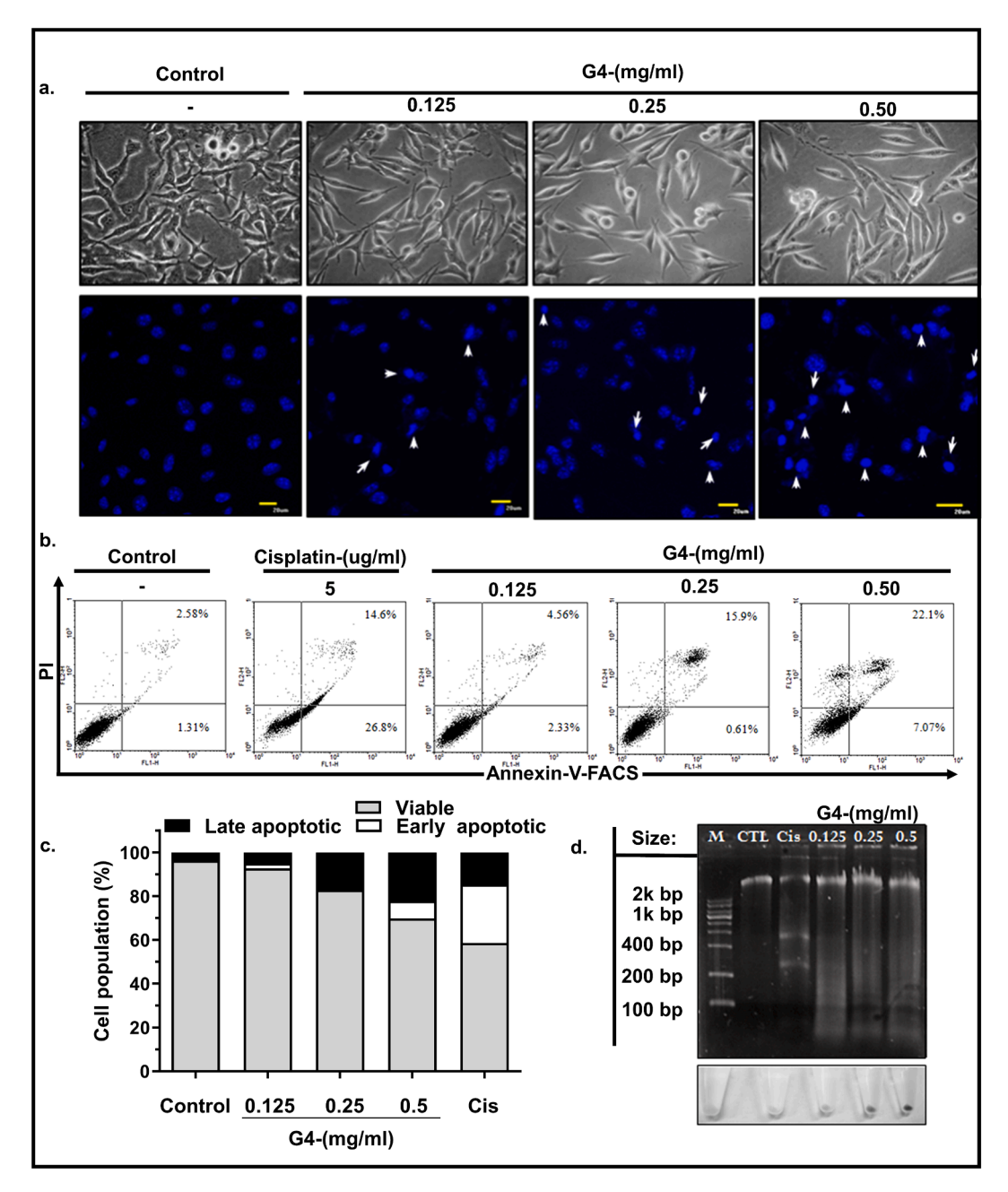


Fig. 5. Analysis of apoptotic features in B16F10 cells following treatment with G4. (A) Morphological alterations in B16F10 cells following treatment with G4 at concentrations of 0.125, 0.25, and 0.5 mg/mL for 24 h, compared to controls. Cells treated with G4 displayed a shrunken appearance, accompanied by chromatin condensation (highlighted by white arrowheads in the lower right panel). Scale bars represent 20  $\mu$ m. (B) Representative dual parametric dot plots illustrating PI fluorescence (y-axis) versus Annexin V-FITC fluorescence (x-axis). (C) Bar graphs showing the percentages of viable, early apoptotic, and late apoptotic cells. (D) Observation of DNA fragmentations in B16F10 cells treated with G4, as visualized by DNA gel electrophoresis.

that the apoptosis induced by G4 in B16F10 melanoma cells is tied to variations in the expression of pro-apoptosis and cell cycle regulatory proteins, underscoring the potential mechanisms that drive the apoptotic effects of the G4 extract.

## 3.7. Xenograft assay

To assess the anti-cancer activity of G4 in vivo, we next utilized a B16F10 melanoma xenograft model in BALB/nu/nu nude mice. B16F10 cells were injected into 5-week-old mice at a concentration of 1 x  $10^6$  cells per mouse. This was followed by the oral administration of G4 at a dose of 175 mg/kg/day over a four-week period. Our data showed that G4 had significant in vivo anti-tumor effects in the B16F10 melanoma

xenograft model (Fig. 7 A). The tumor volume in the G4-treated group was noticeably smaller compared to that in the control groups (Fig. 7 D). Additionally, after euthanizing the mice, tumor weights were determined. There was a pronounced reduction in tumor weight for the G4-treated mice (Fig. 7 B). Importantly, the body weights of mice in both the G4-treated and control groups were similar, with no significant variances detected (Supplementary Fig. S3). This suggests that G4 extract administration did not significantly affect the overall body weight of the mice. Our results highlight that G4 extract has strong anticancer effects in a murine melanoma model. The pronounced reduction in both tumor volume and weight, along with the lack of adverse effects on body weight, emphasize the potential of G4 as a therapeutic option for melanoma treatment.

а

b

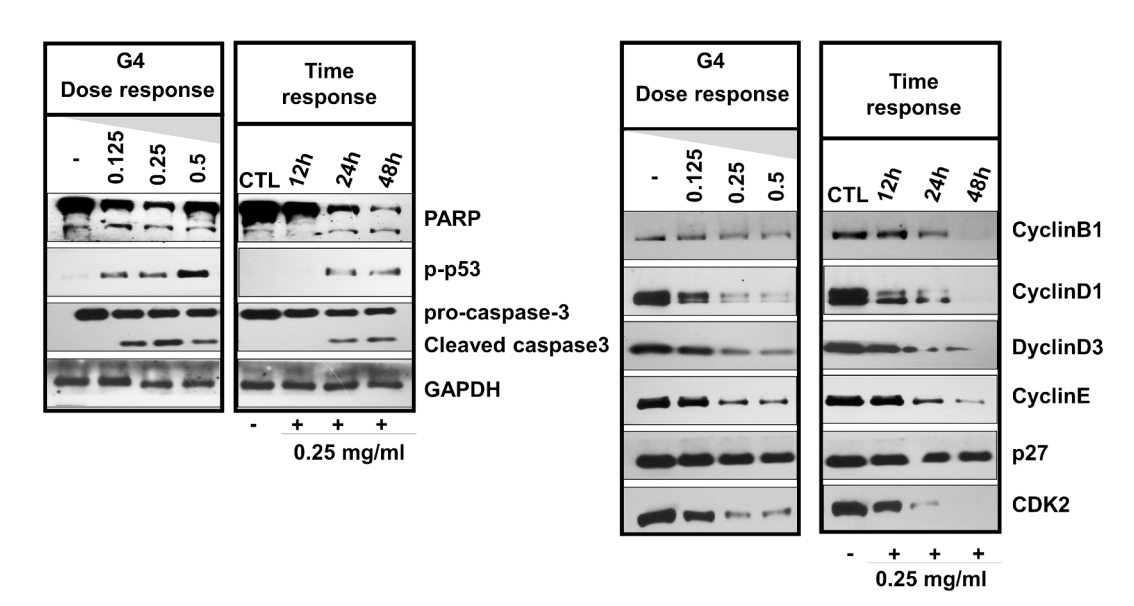


Fig. 6. G4-mediated modulation of apoptosis and cell cycle regulatory proteins, assessed through western blot analysis in a dose- and time-dependent manner. (A) Western blot analysis of apoptotic markers, including activated PARP and activated p53, demonstrating dose- and time-dependent changes. (B) Decreased expression levels of cyclin B1, cyclin D3, cyclin E, and CDK2 following G4 treatment.

#### 4. Discussion

Melanoma, distinguished by its aggressive nature, high metastatic potential, and resistance to conventional treatments, underscores the need for novel therapeutic avenues. Multi-herbal formulations, rooted in traditional medicine, have emerged as promising sources for discovering novel cancer preventive and therapeutic agents (Kaur et al., 2019; Oyungerel et al., 2015). Herbal extracts, renowned for their wide spectrum of biological activities and minimal toxicity, stand as a promising reservoir of potential anti-cancer agents (Kiyohara et al. (2004)). Over 60 % of anti-cancer drugs find their origins in the plant kingdom (Cragg and Newman, 2005; Si et al., 2020). This study aimed to evaluate the anti-melanoma potential of the G4 extract, derived from a multi-herb formulation with historical significance in Mongolian folk medicine (MFM) and Traditional Kazakh medicine (TKM). Despite limited existing reports on these materials, our study represents the inaugural effort to scrutinize the effects of these extracts on B16F10 melanoma cells (Bayarmaa et al., 2018; Cheriet et al., 2020). Our findings demonstrate the anti-cancer effects of the G4 extract, including the promotion of apoptosis, induction of cell cycle arrest, and inhibition of migration and angiogenesis in B16F10 cell lines in vitro. Treatment with the G4 extract resulted in a dose and time-dependent reduction in cell proliferation (Fig. 1 and Fig. 2 A) and migration (Fig. 3 D) in B16F10 melanoma cells. Microscopic examination after 24 h of G4 treatment revealed signs of apoptosis in B16F10 cell lines, characterized by nuclear blebbing and notable nuclear fragmentation (Fig. 5 A). These observations, including nuclear fragmentation and the maintenance of apoptotic body structure, suggest that G4 treatment initiates apoptosis, marked by distinct morphological alterations (Galluzzi et al., 2018).

To further validations of inductions of apoptosis, we evaluated DNA fragmentation, a hallmark of apoptotic cell death (Galluzzi et al., 2018; Kiddane et al., 2022). Cells exposed to varying concentrations of G4 extract underwent genomic DNA isolation followed by analysis using agarose gel electrophoresis. Our experimental findings showcased a distinct ladder pattern in G4-treated cells after 24 h relative to the control cells (Fig. 5 D, Supplementary Fig. S1), signifying that G4 potently induces apoptosis in B16F10 cells. We then examined the correlation between apoptotic induction and cell cycle phases by

conducting flow cytometry on cells treated with G4 at different concentrations (0.125, 0.25, and 0.5 mg/ml). The morphological alterations in the cellular nucleus (Fig. 5 A), and flow cytometric assessments of cell cycle phase results (Fig. 5 B) provided corroborative evidence. Furthermore, our results highlighted the anti-angiogenic potential of the G4 extract, suggesting a potential anti-metastasis effect in an ex-vivo aortic ring assay model (Fig. 4), because micro-vessel outgrowth is important factor of melanoma spreading. Additionally, we utilized an invivo xenograft mouse model, orally administering G4 (175 mg/kg/day) to nude mice inoculated with B16F10 cells. The average tumor volume and weight were notably reduced in the G4-treated group (Fig. 7). In our preliminary investigation, the G4 extract exhibited non-toxicity in mice, evident for up to 21 days post-treatment. This was manifested by stable weight maintenance and the absence of clinical symptoms, such as diarrhea. These findings underscore the potential therapeutic value of the G4 extract in cancer management. Finally, we identified potential volatile compounds in G4 extract using GC-MS (Supplementary Fig. S1) and in the Table S1 listed chemical components of the extract. Nevertheless, the specific compounds accountable for inducing cell death and the overall therapeutic efficacy of this treatment remain to be clarified. As a result, continued investigation of the G4 extract and its components is essential.

### **Study limitations**

First, this study employed a single cell line, B16F10. Second, given that other anti-cancer mechanisms exist, additional studies are essential to identify the effector compounds. Nevertheless, these findings may serve as a reference in cancer medicine and traditional medicine, as this investigation was the inaugural effort to showcase the anti-melanoma effects of the G4 formulation derived from selected traditional medicinal plants in a mouse xenograft model using the B16F10 cell.

## Conclusion

In conclusion, our in vitro data demonstrated that the G4 extract can induce cytotoxicity via the apoptosis pathway in B16F10 cells. *In vivo*, the oral administration of G4 extract reduced the melanoma tumor mass,

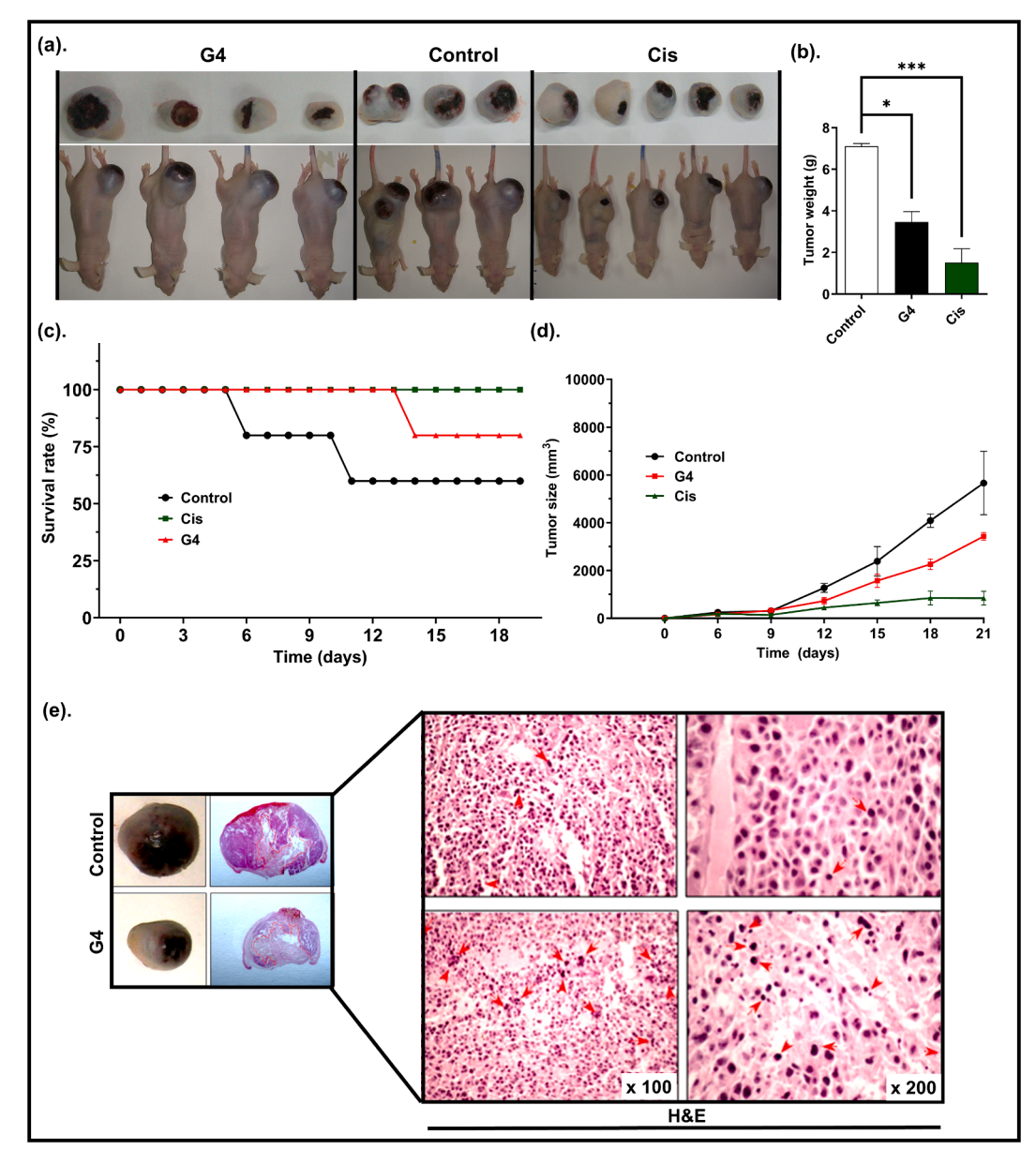


Fig. 7. G4 inhibited tumor growth in a xenograft mouse model. B16F10 cells were injected into 5-week-old BALB/nu/nu nude mice at a concentration of  $1x10^6$  cells per mouse. Mice were administered an oral dose of G4 at 175 mg/kg/day. (A) Solid tumors in the G4-treated group were notably smaller compared to those in the control group. (B) tumor weight, G4 treatment significantly reduced. (C) Survival rate of xenograft mice in the three groups (n = 15 for each group) and (D) tumor size. Values are represented as mean  $\pm$  SD (from triplicate measurements). \*, P < 0.05; \*\*, P < 0.01; \*\*\*\*, P < 0.001; \*\*\*\*\*, P < 0.0001; ns, non-significantly different compared to untreated controls.

suggesting a significant anticancer effect and highlighting the potential to investigate effector molecules involved in this action.

#### **Funding sources**

The study was financially supported by the Mongolian Science and Technology Foundation. Science and technology project (SHUUZ-2017/17).

## CRediT authorship contribution statement

Yerkegul Dauletkhan: Writing – original draft, Visualization, Formal analysis. Tae Young Han: . Janbolat Ashim: Writing – review & editing. Shukherdorj Baasanmunkh: . Altantsetseg Khajidsuren: Data curation, Software, Visualization. Wookyung Yu: Writing – review & editing. Purevjargal Naidansuren: Writing – review & editing.

**Uteubayeva Gulzada:** Conceptualization, Funding acquisition, Project administration, Resources, Supervision, Validation, Writing – review & editing. **Kang Duk Choi:** Conceptualization, Funding acquisition, Project administration, Resources, Supervision, Validation, Writing – review & editing. **Baatartsogt Oyungerel:** Conceptualization, Funding acquisition, Project administration, Resources, Supervision, Validation, Writing – review & editing.

## **Declaration of competing interest**

The authors declare that they have no known competing financial interests or personal relationships that could have appeared to influence the work reported in this paper.

#### Data availability

The data that has been used is confidential.

#### Acknowledgements

This study is a part of the Ph.D. thesis of the first author. The study was financially supported by the Mongolian Science and Technology Foundation. Science and technology project (SHUUZ-2017/17).

#### Appendix A. Supplementary data

Supplementary data to this article can be found online at https://doi.org/10.1016/j.crbiot.2024.100217.

#### References

- Antohe, M., Nedelcu, R.I., Nichita, L., Popp, C.G., Cioplea, M., Brinzea, A., Hodorogea, A., Calinescu, A., Balaban, M., Ion, D.A., Diaconu, C., Bleotu, C., Pirici, D., Zurac, S.A., Turcu, G., 2019. Tumor infiltrating lymphocytes: The regulator of melanoma evolution (Review). Oncol. Lett. 17, 4155–4161. https://doi. org/10.3892/ol.2019.9940.
- Arnold M, Singh D, Laversanne M, Vignat J, Vaccarella S, Meheus F, Cust AE, de Vries E, Whiteman DC, Bray F, 2022. Global Burden of Cutaneous Melanoma in 2020 and Projections to 2040. JAMA Dermatol. 158(5), 495-503. doi: jamadermatol.2022.0160.
- Baasanmunkh, S., Urgamal, M., Oyuntsetseg, B., Sukhorukov, A.P., Tsegmed, Z., Son, D. C., Erst, A., Oyundelger, K., Kechaykin, A.A., Norris, J., Kosachev, P., Ma, J.-S., Chang, K.S., Choi, H.J., 2022. Flora of Mongolia: annotated checklist of native vascular plants. PhytoKeys 192, 63–169. https://doi.org/10.3897/phytokeys.192.79702.
- J. Bao DIng, R., Zou, L., Zhang, C., Wang, K., Liu, F., Li, P., Chen, M., Wan, J.B., Su, H., Wang, Y., He, C., Forsythiae Fructus Inhibits B16 Melanoma Growth Involving MAPKs/Nrf2/HO-1 Mediated Anti-Oxidation and Anti-Inflammation Am. J. Chinese Med. 44 2016 1043 1061 10.1142/S0192415X16500580.
- Barbieri, A., Quagliariello, V., Del Vecchio, V., Falco, M., Luciano, A., Amruthraj, N.J., Nasti, G., Ottaiano, A., Berretta, M., Iaffaioli, R.V., Arra, C., 2017. Anticancer and anti-inflammatory properties of ganoderma lucidum extract effects on melanoma and triple-negative breast cancer treatment. Nutrients 9. https://doi.org/10.3390/ nu9030210.
- Bayarmaa, G.A., Lee, N.N., Kang, H.D., Oyuntsetseg, B., Moon, H.K., 2018. Micropropagation of the Mongolian medicinal plant Zygophyllum potaninii via somatic embryogenesis. Plant Biotechnol. Rep. 12, 187–194. https://doi.org/ 10.1007/s11816-018-0484-9
- Bellacen, K., Lewis, E.C., 2009. Aortic Ring Assay. J. vis. Exp. https://doi.org/10.3791/1564.
- Chambers, A.F., Groom, A.C., MacDonald, I.C., 2002. Dissemination and growth of cancer cells in metastatic sites. Nat. Rev. Cancer. https://doi.org/10.1038/nrc865.
- Cheriet, T., Ben-Bachir, B., Thamri, O., Seghiri, R., Mancini, I., 2020. Isolation and biological properties of the natural flavonoids pectolinarin and pectolinarigenin—a review. Antibiotics 9, 417. https://doi.org/10.3390/antibiotics9070417.
- Cragg, G.M., Newman, D.J., 2005. Plants as a source of anti-cancer agents.
  J. Ethnopharmacol. 100, 72–79. https://doi.org/10.1016/j.jep.2005.05.011.
- Dzhumagaliyeva, K.V., Sarmurzina, N., Kayrgaliyeva, G., 2020. History of traditional medicine of Kazakh people. History Sciences 2, 117–126. https://doi.org/10.37313/ 2658-4816-2020-2-1-117-126.
- Feng, X., Cao, S., Qiu, F., Zhang, B., 2020. Traditional application and modern pharmacological research of *Artemisia annua* L. Pharmacol. Ther. 216, 107650 https://doi.org/10.1016/j.pharmthera.2020.107650.
- Galluzzi, L., Vitale, I., Aaronson, S.A., Abrams, J.M., Adam, D., Agostinis, P., Alnemri, E. S., Altucci, L., Amelio, I., Andrews, D.W., Annicchiarico-Petruzzelli, M., Antonov, A. V., Arama, E., Baehrecke, E.H., Barlev, N.A., Bazan, N.G., Bernassola, F., Bertrand, M.J.M., Bianchi, K., Blagosklonny, M.V., Blomgren, K., Borner, C., Boya, P., Brenner, C., Campanella, M., Candi, E., Carmona-Gutierrez, D., Cecconi, F., Chan, F.K.M., et al., 2018. Molecular mechanisms of cell death: Recommendations of the Nomenclature Committee on Cell Death 2018. Cell Death Differ. https://doi.org/10.1038/s41418-017-0012-4.
- Gendaram, O., 2017. Anti-oxidative, acetylcholinesterase and pancreatic lipase inhibitory activities of compounds from Dasiphora fruticosa, Myricaria alopecuroides and Sedum hybridum. Mong. J. Chem. 17, 42–49. https://doi.org/ 10.5564/mjc.v17i43.746.
- Gray-Schopfer, V., Wellbrock, C., Marais, R., 2007. Melanoma biology and new targeted therapy. Nature. https://doi.org/10.1038/nature05661.
- Halder, B., Singh, S., Thakur, S.S., 2015. Withania somnifera root extract has potent cytotoxic effect against human malignant melanoma cells. PLoS One 10. https://doi. org/10.1371/journal.pone.0137498.
- Harhaji Trajkovic, L.M., Mijatovic, S.A., Maksimovic-Ivanic, D.D., Stojanovic, I.D., Momcilovic, M.B., Tufegdzic, S.J., Maksimovic, V.M., Marjanovi, Z.S., Stosic-Grujicic, S.D., 2009. Anticancer properties of ganoderma lucidum methanol extracts in vitro and in vivo. Nutr. Cancer 61, 696–707. https://doi.org/10.1080/ 01635580902898743.

- Iwase, S., Yamaguchi, T., Miyaji, T., Terawaki, K., Inui, A., Uezono, Y., 2012. The clinical use of Kampo medicines (traditional Japanese herbal treatments) for controlling cancer patients' symptoms in Japan: A national cross-sectional survey. BMC Complement Altern Med 12. https://doi.org/10.1186/1472-6882-12-222.
- P. Kaur M. Robin R.G., Singh, B., Arora, S., Development of aqueous-based multi-herbal combination using principal component analysis and its functional significance in HepG2 cells BMC Complement Altern Med 19 2019 10.1186/s12906-019-2432-9.
- Kiddane, A.T., Kang, M.J., Ho, T.C., Getachew, A.T., Patil, M.P., Chun, B.S., Kim, G.D., 2022. Anticancer and apoptotic activity in cervical adenocarcinoma hela using crude extract of *Ganoderma applanatum*. Curr Issues Mol. Biol. 44, 1012–1026. https://doi.org/10.3390/cimb44030067.
- Kim, M.K., Bang, C.Y., Kim, M.Y., Lee, J.H., Ro, H., Choi, M.S., Kim, D.I., Jang, Y.P., Choung, S.Y., 2016. Traditional herbal prescription LASAP-C inhibits melanin synthesis in B16F10 melanoma cells and zebrafish. BMC Complement Altern Med 16. https://doi.org/10.1186/s12906-016-1209-7.
- Kim, H.-Y., Lee, S.-W., Choi, S.-K., Ashim, J., Kim, W., Beak, S.-M., Park, J.-K., Han, J.E., Cho, G.-J., Ryoo, Z.Y., Jeong, J., Lee, Y.-H., Jeong, H., Yu, W., Park, S., 2023.
  Veratramine Inhibits the Cell Cycle Progression, Migration, and Invasion via ATM/ ATR Pathway in Androgen-Independent Prostate Cancer. Am. J. Chin. Med. 1–25 https://doi.org/10.1142/S0192415X2350060X.
- Kim, W., Yeo, D.-Y., Choi, S.-K., Kim, H.-Y., Lee, S.-W., Ashim, J., Han, J.E., Yu, W., Jeong, H., Park, J.-K., Park, S., 2022. NOLC1 knockdown suppresses prostate cancer progressions by reducing AKT phosphorylation and β-catenin accumulation. Biochem Biophys Res Commun 635. https://doi.org/10.1016/j.bbrc.2022.10.038.
- Kiyohara, H., Matsumoto, T., Yamada, H., 2004. Combination Effects of Herbs in a Multiherbal Formula: Expression of Juzen-taiho-to's Immuno-modulatory Activity on the Intestinal Immune System, eCAM.
- Kumari, S., Seth, A., Sharma, S., Attri, C., 2021. A holistic overview of different species of Potentilla, a medicinally important plant, along with their pharmaceutical significance: A review. J Herb Med 29, 100460. https://doi.org/10.1016/j. hermed.2021.100460.
- Majtnerová, P., Roušar, T., 2018. An overview of apoptosis assays detecting DNA fragmentation. Mol. Biol. Rep. 45, 1469–1478. https://doi.org/10.1007/s11033-018-4258-9.
- Nurlybekova, A., Kudaibergen, A., Kazymbetova, A., Amangeldi, M., Baiseitova, A., Ospanov, M., Aisa, H.A., Ye, Y., Ibrahim, M.A., Jenis, J., 2022. Traditional Use, Phytochemical Profiles and Pharmacological Properties of *Artemisia* Genus from Central Asia. Molecules 27, 5128. https://doi.org/10.3390/molecules27165128.
- Oyungerel, B., Chung, S., Yoon, D.Y., Han, T.Y., Han, I.Y., Kweon, K.T., Kim, K.M., Jeon, G.J., Choi, K.D., 2015. C5 extract induces apoptosis in B16F10 murine melanoma cells through extrinsic and intrinsic apoptotic pathways and Sub-G1 phase arrest. Trop. J. Pharm. Res. 14, 967–976. https://doi.org/10.4314/tjpr. v14i6 5
- Pijuan, J., Barceló, C., Moreno, D.F., Maiques, O., Sisó, P., Marti, R.M., Macià, A., Panosa, A., 2019. In vitro Cell Migration, Invasion, and Adhesion Assays: From Cell Imaging to Data Analysis. Front. Cell. Dev. Biol. 7 https://doi.org/10.3389/ fcell.2019.00107.
- Purushotham, G., Padma, Y., Nabiha, Y., Venkata Raju, R.R., 2016. In vitro evaluation of anti-proliferative, anti-inflammatory and pro-apoptotic activities of the methanolic extracts of Andrographis nallamalayana Ellis on A375 and B16F10 melanoma cell lines. 3 Biotech 6. doi: 10.1007/s13205-016-0529-0.
- Qamar, M., Akhtar, S., Ismail, T., Wahid, M., Ali, S., Nazir, Y., Murtaza, S., Abbas, M.W., Ziora, Z.M., 2022. Syzygium cumini (L.) Skeels extracts; in vivo anti-nociceptive, anti-inflammatory, acute and subacute toxicity assessment. J. Ethnopharmacol. 287 https://doi.org/10.1016/j.jep.2021.114919.
- D. Schadendorf A.C.J. van Akkooi C. Berking K.G. Griewank R. Gutzmer A. Hauschild A. Stang A. Roesch S. Ugurel Melanoma, Melanoma Lancet 392 2018 10151 10.1016/S0140-6736(18)31559-9.
- Schneider, C.A., Rasband, W.S., Eliceiri, K.W., 2012. NIH Image to ImageJ: 25 years of image analysis. Nat. Methods. https://doi.org/10.1038/nmeth.2089.
- Si, L., Yan, X., Wang, Y., Ren, B., Ren, H., Ding, Y., Zheng, Q., Li, D., Liu, Y., 2020. Chamaejasmin B Decreases Malignant Characteristics of Mouse Melanoma B16F0 and B16F10 Cells. Front. Oncol. 10 https://doi.org/10.3389/fonc.2020.00415.
- Šmejkal, K., Malaník, M., Zhaparkulova, K., Sakipova, Z., Ibragimova, L., Ibadullaeva, G., Žemlička, M., 2016. Kazakh Ziziphora species as sources of bioactive substances. Molecules. https://doi.org/10.3390/molecules21070826.
- Soares, S.S., Bekbolatova, E., Cotrim, M.D., Sakipova, Z., Ibragimova, L., Kukula-Koch, W., Giorno, T.B.S., Fernandes, P.D., Fonseca, D.A., Boylan, F., 2019. Chemistry and pharmacology of the Kazakh crataegus amanuensis park: An Asian herbal medicine. Antioxidants 8. https://doi.org/10.3390/antiox8080300.
- Tang, Z., Li, W., Xie, H., Jiang, S., Pu, Y., Xiong, H., 2021. Taohong Siwu-Containing Serum Enhances Angiogenesis in Rat Aortic Endothelial Cells by Regulating the VHL/HIF-1 α /VEGF Signaling Pathway. Evid. Based Complement. Alternat. Med. 2021 https://doi.org/10.1155/2021/6610116.
- Tomczyk, M., Latté, K.P., 2019. Potentilla—A review of its phytochemical and pharmacological profile. J. Ethnopharmacol. 122, 184–204. https://doi.org/ 10.1016/j.jep.2008.12.022.
- Tsevegsuren, N., Edrada, R.A., Lin, W., Ebel, R., Torre, C., Ortlepp, S., Wray, V., Proksch, P., 2007. Biologically active natural products from Mongolian medicinal plants *Scorzonera divaricata* and *Scorzonera pseudodivaricata*. J. Nat. Prod. 70, 962–967. https://doi.org/10.1021/np070013r.

- Wang, Y., Lv, J., Cheng, Y., Du, J., Chen, D., Li, C., Zhang, J., 2015. Apoptosis induced by Ginkgo biloba (EGb761) in melanoma cells is Mcl-1-dependent. PLoS One 10. https://doi.org/10.1371/journal.pone.0124812.
- Wurchaih, H., Menggenqiqig, K., 2019. Medicinal wild plants used by the Mongol herdsmen in Bairin Area of Inner Mongolia and its comparative study between TMM and TCM. J. Ethnobiol. Ethnomed. 15 https://doi.org/10.1186/s13002-019-0300-9.
- Yang, Y., Li, S., Teixeira da Silva, J.A., Yu, X., Wang, L., 2020. Characterization of phytochemicals in the roots of wild herbaceous peonies from China and screening for medicinal resources. Phytochemistry 174, 112331. https://doi.org/10.1016/j. phytochem.2020.112331.

#### **Further reading**

- Y. Bak S. Ham H. Seung C. Kang-Duk Tae-Young, Il-Young H., Do-Young Y., A1E inhibits proliferation and induces apoptosis in NCI-H460 lung cancer cells via extrinsic and intrinsic pathways Mol. Biol Rep. 40 2013 4507 4519 10.1007/s11033-013-2544-0.
- Erdei, E., Torres, S.M., 2014. A new understanding of the epidemiology of melanoma. Expert Rev. Anticancer Ther. 10, 1811–1823. https://doi.org/10.1586/era.10.170.
- G. Seo H.-O. Pae G.-S. Oh K.-Y. Chai Y.-G. Yun Chung', H.-T., Jang, K.K., Kwon, T.-O., Ethyl Acetate Extract of the Stem Bark of Cudrania Tricuspidata Induces Apoptosis in Human Leukemia HL-60 Cells Am. J. Chin. Med. 2001.